Work Package 2.4

Part I:

Land Cover Change Analysis in Metro Manila and Marikina Watershed Philippines (2009-2018)

Abstract

This part aims to analyze land cover change of Metro Manila from 2009 to 2018. We collected and pre-processed multi-temporal satellite images from Landsat 5, 7, and 8 and Sentinel 2. The pre-processed images were classified using pixel-based supervised classification techniques including Support Vector Machine (SVM), Neural Network (NN), Random Forest (RF) and Maximum Likelihood Classifier (MLC). The average overall accuracy of NN was roughly 1% higher than SVM and RF and about 8% higher than ML. Less than 33% of the study site's land cover changed. Built-up area gained 10.3 % in nine years with urban expansion rate doubling in the past four years. Vegetation cover lost 12.4% in the same period. Tree cover dropped from 48.9% in 2009 to 42.64% in 2014 but slightly recovered to 43.4% in 2018 which is slightly higher than the 42.8% built-up cover in 2018. Major drivers of land cover change here are urban development, agriculture and mining as their rate exceeded reforestation rate. Our results call for strengthening of the implementation of the UMRB Protected Landscape law to protect and preserve the vegetal cover in the study site. This also calls for equitable land use planning for the watershed and proper implementation for sustainable resource use as less space becomes available for the competing demands.

Introduction

Remote Sensing has proven to be one of the useful tools in studying LCC (Toure, Stow, Shih, Weeks, & Lopez-Carr, 2018). Several supervised and unsupervised classification techniques have been developed and can be used for land cover classification. Below are some of the algorithms for land cover classification.

Maximum Likelihood

ML is said to be the most commonly used classification algorithm because of its easy and fast execution (Karan & Samadder, 2018). It is a performant algorithm as shown in the results of (Priyadarshini, Kumar, Rahaman, & NitheshNirmal, 2018) who compared Maximum Likelihood Classifier, Minimum Distance, Parallelipiped, Support Vector Machine, ISO Data, and K-means on Sentinel 2 image for classes including river sand, forest, urban, river, mountain, scrub, and crop. Their results revealed that MLC had the highest accuracy among the tested algorithms (Priyadarshini, Kumar, Rahaman, & NitheshNirmal, 2018). MLC works by the logic of Bayes theorem computing the probability of a pixel belonging to a class based on the statistical parameters including

the mean and covariance matrix of the class training sites (Ahmad & Quegan, 2012). Maximum Likelihood classifier works under the assumption that the classes have a normally distributed spectra (Meng, Currit, Wang, & Yang, 2010; Karan & Samadder, 2018).

Support Vector Machine

SVM, according to Ustuner et al. (2015), is a learning algorithm falling under the non-parametric classifiers. SVM uses the training data values for generating a prediction model for a pixel (Hsu et al., 2010) then looks for an optimization solution (Karan & Samadder, 2018). For classification, SVM looks for the hyperplane that maximizes the separation between trained categories (Murayama, Estoque, Subasinghe, Hou, & Gong, 2015; Karan & Samadder, 2018). SVM selects the hyperplanes, also called support vectors, that have the largest separation from the nearest training data points (Griffiths et al., 2010; Murayama, Estoque, Subasinghe, Hou, & Gong, 2015).

As an advanced classification algorithm, researchers reported successful image classification using SVM. Karan & Samadder (2018) compared ML, NN, SVM, Mahalanobis, Minimum Distance, and Spectral Angle Mapper and learned that SVM (95%), NN (91%), and ML (84%) produced the most accurate land cover classification for VHR image. Deilmai, Ahmad, & Zabihi (2014) compared MLC with SVM in classifying forests, oil palm, urban area, water, and rubber and recommended to use SVM producing 91.67% overall accuracy compared with the 78.33% accuracy obtained through Maximum Likelihood. Jimenez, Vilchez, Gonzales, & Marceleno Flores, (2018) compared SVM, MLC and ANN with SVM having the highest kappa index of more than 85%.

Neural Network

Neural Network is another machine learning algorithm. It acts like an interconnected web of neurons. This algorithm is composed of input, hidden and output layers. Input layer provides the information necessary in training the algorithm. Hidden layers compute the weights and biases together with the input information to produce an output. Multiple hidden layers may be assigned based on the number of inputs and outputs. All the outputs of each node are added up and fitted to the activation function that may be selected (logistic, hyperbolic, RELU, leaky RELU, etc.). Training happens through backward propagation process in which the error (root mean square) of the output and estimated output (Richards and Jia 2006; Karan & Samadder, 2018). The algorithm learns by adjusting the weights to lower the RMS. Several parameters may affect the quality of classification results. These parameters include training threshold contribution which determines how much influence the internal weight may have on node activation. Training rate also affects the results as this controls the weight adjustment. Training momentum controls the direction of weight change. Training will

go on repeatedly until it falls below an assigned acceptable RMS or when it reaches the indicated number of training iterations (Karan & Samadder, 2018).

Random Forest

Random Forest classifies an image using a collection of decision trees (Murayama, Estoque, Subasinghe, Hou, & Gong, 2015). A decision tree separates the data into classes by looking at the dataset's values for a given variable. Random forest starts by selecting a subset from the data in random and in repetition (Karan & Samadder, 2018). A decision tree will be built based on this data subset. The algorithm will randomly choose a variable and split the data according to the value that reduces the entropy in the subset data. Once divided, the data would have a lower entropy. This happens at several decision trees. The user indicates the number of tree nodes to be generated. The algorithm will repeatedly split the data to generate leaf nodes that contain a classification. The final classification is a product of the most number of votes among the decision trees (Karan & Samadder, 2018). Random tree, compared with other advanced supervised classification algorithms require the least number of input parameters (Immitzer et al., 2012). The only input parameter required for Random Forest is the number of trees (Ntree).

Remote sensing for LULCC in Metro Manila

Several researchers have used remote sensing to analyze LULCC in Metro Manila. Taubenbock (2012) studied urban expansion trends of selected major metropolises, including Metro Manila, through object-based and pixel-based classification of multi-temporal Landsat and TerraSAR-X images from 1970s up to 2010. Their results showed that Manila grew more than seven times in a span of 35 years (Taubenbock, et al., 2012). They also noted that Manila, similar to Mexico City and Istanbul exhibited terrain-influenced urban expansion (Taubenbock, et al., 2012). Albino, et al, (2015) used Maximum Likelihood classifier in studying land cover change from 1999 to 2006 in Marikina Subwatershed and Markov Chain to predict the probable land cover in 2020 giving insights on the appropriate land use-related policies and strategies for watershed management.

Estoque, et al., (2018) used remote sensing techniques on Landsat data to monitor the land cover change in La Mesa Watershed which is part of the study site. They found that rehabilitation of the watershed that took place in 1999 increased the forest cover by 557 hectares. Estoque (2017) also studied the land cover change in Metro Manila and in the surrounding northern and southern provinces from 1993 up to 2014 and noted that the rate of urban land expansion decreased in the 2001 to 2009 period and increased again in the following five years. The urban areas expanded and are moving towards the boundaries of Metro Manila. They also projected a continuous increase in urban spaces up to 2030 from the 848.63 km^2 to 1112.27 km^2.

Factors Affecting Land Cover Change

Past research focused on urban expansion affecting land cover change. Another factor affecting land cover change in Metro Manila is the National Greening Program which aimed to reforest more than 1.5 million hectares and ban logging in forests in five years starting 2011.

Another factor influencing land cover change in the study site is mineral extraction. According to MGB records Mineral Production Sharing Agreement (MPSA) increased from 50.2 km^2 in 2015 to 60.6 km^2 in 2019. Most of these Mineral Production Sharing Agreement (MPSA) were approved and have been commercially operating since late 1990s. Three more Mineral Production Sharing Agreement were approved after 2009.

Objective

This paper aims to study the land cover change in Metro Manila in the past nine years using high resolution images, Landsat 5, Landsat 7 and Landsat 8 and Sentinel 2 to update the past studies to analyze the trends and drivers of change. We would like to relate land cover changes with land use-related policies such as reforestation programs, protected landscape proclamation, approval of mining tenements in the area, urban and infrastructure development and agricultural use that could drive land cover transition.

Research methods

Description of the study site

The study site covers Metro Manila and Pasig-Marikina and Manggahan Watershed. This study site, covering a total area of 1,602.79 km^2, is located downstream of Marikina River in the East, Laguna Lake in the South and Manila Bay in the West. This study site consists a portion of the Pasig-Marikina-Laguna de Bay Basin covering a total area of 3,651.50 km^2. The eastern portion covers the Sierra Madre Mountains and forms the upper Marikina Watershed draining through the Marikina River and Pasig River to Manila Bay and to Laguna Lake through Napindan Channel. Flood events usually occurs when these river systems overflow. Flood usually affects the western portion covering a flat to rolling terrain mostly built-up. Expanse of residential areas, major businesses, industries, and institutions pertinent to national economic, political, social, and educational activity of the country occupies these low-lying areas.

Climate Type I and III of the Modified Coronas Classification typifies the climate in the study site. Metro Manila is under the Type I climate that has two different climate – the dry season from November to April and wet season from May to October.

The Marikina Watershed is under the Climate Type III that has three wet months. PAGASA's climatological normal values in Tanay station identify February to April as the driest months. Wet season tend to have more cloud cover so most of the images available for land cover classification are captured during dry season. The amount of rain and the temperature also influence the vegetation health and amount of bare soil that can be detected from the satellite images. Bare soil tends to be more exposed during dry months of March and April. Type III climate may also experience dry months from March to May.

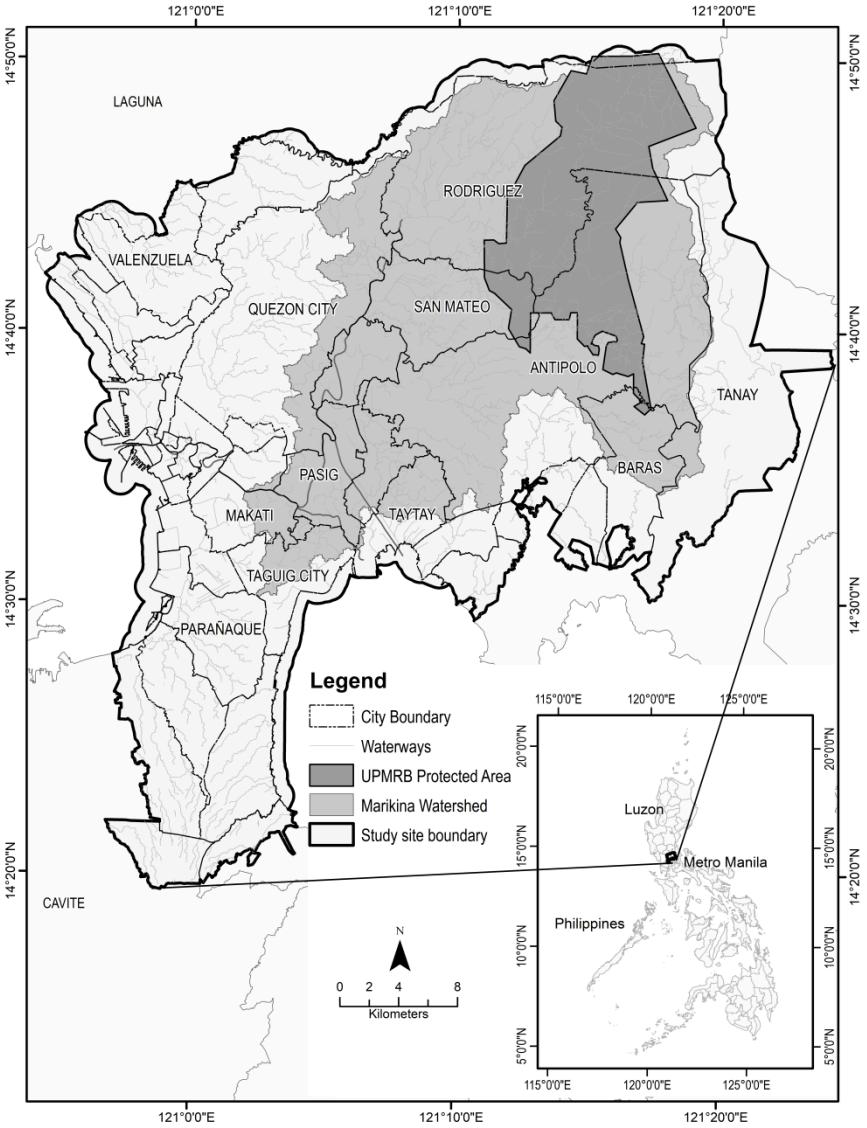

Figure 1. Study site covering Metro Manila and Marikina Watershed

Data

We acquired Level-1 Landsat images and Sentinel-2 images from earthexplorer.usgs.gov and scihub.copernicus.eu, respectively. We used high resolution satellite images from Landsat sensors (TM, ETM+, OLI) and Sentinel 2 images. Images

were selected to cover 2009, 2010, 2014, and 2018. All images were taken during dry season. Visible, Near-Infrared and Mid-Infrared bands of Landsat TM, ETM+ and OLI and Sentinel-2 images were used for land cover classification as these bands are common to the sensors and has the least atmospheric influence.

Table 1: Satellite data used for land cover classification

SATELLITE IMAGE	DATE	SENSOR	Spatial Resolution
LE71160502009336EDC01	12/2/2009	Landsat 7	30
LT05_L1TP_116050_20100127_20161020_01_T1	1/27/2010	Landsat 5	30
LC08_L1TP_116050_20140207_20170426_01_T1	2/7/2014	Landsat 8	30
L1C_T51PTR_A014300_20180319T022847	3/19/2018	Sentinel 2	10-20
L1C_T51PTS_A014300_20180319T022847	3/19/2018	Sentinel 2	10-20
L1C_T51PUS_A014300_20180319T022847	3/19/2018	Sentinel 2	10-20

Methods

Landsat TM, ETM+, OLI and Sentinel 2 images were calibrated to convert the DN values to Top of Atmosphere Reflectance and atmospherically corrected using Dark Object Subtraction 1 (Moran, Jackson, Slater, & Teillet , 1992) to remove the atmospheric brightness and to have a more accurate ground surface reflectance. The image bands were clipped to the study site boundary to reduce processing time and file size and stacked to produce a single image file for processing. Image-to-image registration was performed as needed to ensure that the image pixels are at the same location for all the images as is necessary for multi-temporal comparison. The three Sentinel-2 scenes composing the study site were mosaicked to produce a single image. Sentinel-2 visible bands and NIR having a ground resolution of 10 meters and the SWIR bands having a resolution of 20 meters were resampled using Nearest Neighbor method (Richards, 1999) to 30 meters to match the ground resolution of Landsat images and to avoid inconsistencies caused by differences in image resolution when comparing multi-temporal land cover classification.

Thorough image interpretation and on-screen digitization followed image pre-processing. Here, training sites and ground truth sites were manually digitized for 5 identified classes namely: trees, grass, bare soil, built-up and water of the pre-processed image supplemented by archival images in Google Earth closest capture date to the Landsat and Sentinel-2 images used. Trees were separated from bare soil based on the texture and color. Bare soils training sites are the exposed soil in the quarry sites, construction sites and vacant lots without grass. Built-up areas include the houses, paved surfaces, and buildings. Pixels from various surface water bodies were collected. Training pixels were collected at stratified random sites until sufficient or roughly 0.25% of the total study area was sampled (Noi & Kappas, 2017).

Once sufficient training sites were collected, ROI separability was computed using Jeffries-Matusita Transformed Divergence of Envi 5.3. Computed ROI separability was greater than 1.5 which is means that the classes were separable.

The training sets were used to classify the image using four classifiers: maximum likelihood classification, neural network, support vector machine, and random forest classification. ENVI 5.3 was used to execute maximum likelihood, neural network and support vector machine while R was used to execute random forest classification.

Maximum Likelihood

Maximum Likelihood uses the mean and standard deviation of the training data per band for the classification. It then computes for the covariance matrix to weigh the distance between the pixel mean and that of the training data. ML then computes for the probability equation per class for each pixel and assigns the pixel to the class that has the highest probability. For this classification, the user may assign the probability threshold but we opt not to do so because this would result in unclassified pixels.

Neural Network

In our use of Neural Network, the most common activation function, logistic, was used. Training threshold contribution was set at 0.9 so that the weights were adjusted minimizing the error. Training rate was set at 0.2 to lessen training errors caused by oscillations but keeping the processing time at a minimum. Training momentum was set at the default, 0.9. The training ended when the RMS was below 0.1 or after 1000 iterations. Number of hidden layers was set at default 1 which is the usual number of hidden layers and was recommended by several studies (Kanellopoulos&Wilkinson,1997; Shupe&Marsh,2004 cited in Sharma, et al., 2018).

Random Forest

R was used to execute random forest algorithm due to ease of utility and availability. We installed rgdal package which reads the shape file inputs containing the location of training points. Other packages such as sp and raster packages were also installed to enable spatial processes necessary in preparing and analyzing the input data for random forest classification. Raster data of the six selected image bands was extracted to generate a dataframe containing the training sites represented as points. Breiman and Cutler's Random Forests for Classification and Regression (randomForest) package version 4.6-14 was used to execute the algorithm on the input datasets. We

assigned 500 Ntrees as recommended by Begiu & Dragut (2016). Finally, the land cover class was predicted per pixel.

Support Vector Machine

We selected the Radial Basis Function as the Kernel type with an error penalty weight of 100 and Gamma value of 0.167 as it was superior among the tested kernel types according to the study of Yang (2011). We used Envi 5.3 to execute SVM algorithm.

Accuracy Assessment

Confusion matrix which is a common method for computing classification accuracy was used to assess the results. The groundtruth pixels were compared with the classified image and overall accuracy, kappa value, commission and omission error and producer's and user's accuracies were computed.

Post Processing

For the 2009 and 2010 images, clouds were removed post-classification by replacing the pixels classified as either cloud or shadow from 2009 image with the classified non-cloud and non-shadow pixels from 2010. For this process, the key is finding two sets of image with the least time difference and where the clouds are located in different places.

After classification, accuracy assessment was performed using confusion matrix to determine the performant classifier. The classified area per class was considered in the computation of the accuracy assessment to reduce bias towards the class with the most ROI pixel. GIS was used to analyze the changes and to compute for the land cover transitions.

Results and Discussion

Land Cover Classification Accuracy Assessment

All the algorithms produced satisfactory land cover classifications with an accuracy of at least 81.6%. Table 3 shows the overall accuracy and Kappa Index of the classifiers per analysis year. NN and SVM had the highest overall accuracy of at least 93.0% and 93.6%, respectively. RF also had high overall accuracy (at least 91.5%). ML was able to classify the images but had lower overall accuracy (at least 81.6%) compared with the other algorithms.

For the three analysis years, NN had an average of 94.03% overall accuracy, greater than SVM with 93.7%. RF, with an average overall accuracy of 92.83, closely followed the performance of NN and SVM. On the other hand, the average overall accuracy of ML is 86.10%. These results showed that the machine learning algorithms overall performed better than the parametric classifier.

Table 2: Overall accuracy and Kappa Index of multi-temporal image classified using MLC, NN, RF, and SVM

	OVERALL ACCURACY (OA)				KAPPA			
YEAR	ML	NN	RF	SVM	ML	NN	RF	SVM
2009	89.40	93.00	91.50	93.60	0.83	0.89	0.86	0.89
2014	81.60	95.50	95.50	93.40	0.75	0.93	0.93	0.90
2018	87.30	93.60	91.50	94.10	0.81	0.90	0.87	0.90
AVERAGE	86.10	94.03	92.83	93.70	0.79	0.90	0.89	0.90

NN, RF and SVM had greater than 95.9% PA and UA for tree and water classes (Table 3). ML was inconsistent in classifying tree and water. NN (>89.7% PA and UA) performed better at classifying built-up areas than RF (>88.7%) and SVM (>86.7) and ML (79.6%). Built-up was more difficult to classify than water and trees due to the heterogenous nature of built-up materials, cited as a major hindrance in urban land cover classification (Forster, 1983, 1985; Small, 2003, 2005; Weng & Liu, 2007, Small 2005). Taubenbock, et al., (2012) also noted the “intraurban spectral variability” and “interurban socio-economic and environmental variability” that makes urban land cover classification more challenging. ML had the lowest PA and UA for built-up also due to the variability of materials in the urban land cover class. This variability did not fit with the Gaussian distribution assumption for the computation and poses challenge to ML (Forster, 1983, 1985; Small, 2003, 2005; Weng & Liu, 2007, Small 2005; Taubenbock, et al., 2012) Previous studies explained that the diverse reflectances from urban features adds bias to the statistical input and results in some inaccuracies in the Bayesian-based classification (Meng, Currit, Wang, & Yang, 2010).

For grass, SVM had the highest PA and UA of at least 78.3%, far higher than RF (>72%), NN (>62.1) and ML (>52.9). All algorithms produced inaccuracies in classifying bare soil across all analysis years producing the lowest PA and UA of 15% and 39.1%, respectively. Difficulty in accurately classifying bare soil was also experienced by Lichtblau & Oswald (2019) who noted that bare soil can be confused with roads and grass in shaded areas as the spectra of bare soil is in between that of vegetation and impervious surfaces. We compared the spectra of bare soil training site with built-up spectra and observed slight difference between the two spectra. This could confuse the classifier and lead to low accuracy for bare soil class. Another reason for the

inaccurate bare soil classification was the selection of the training site. The training site for bare soil was collected in areas with exposed soil which are usually in construction and quarry sites.

Table 3: Producer's and User's accuracy of images classified using different classifiers per class

		ML		NN		RF		SVM	
	CLASS	PA	UA	PA	UA	PA	UA	PA	UA
	BARE	22.5	47.9	19.5	95.5	30.7	65.0	15.0	39.1
	GRASS	100.0	52.9	100.0	62.1	100.0	72.0	100.0	78.3
	HIBU	87.0	89.1	98.7	92.7	89.7	90.6	93.7	91.6
	TREE	98.4	98.8	98.9	99.3	99.3	95.9	100.0	97.7
2009	WATER	81.8	100.0	97.7	100.0	99.0	99.9	98.9	100.0
	BARE	84.5	45.1	32.5	63.2	34.6	78.3	20.2	64.5
	GRASS	99.0	68.6	98.4	100.0	98.7	100.0	96.4	95.5
	HIBU	83.5	87.6	97.7	90.5	98.5	91.4	97.7	86.7
	TREE	76.0	99.8	98.8	99.6	98.0	99.4	98.9	99.2
2014	WATER	58.0	100.0	99.3	99.9	100.0	99.5	100.0	99.9
	BARE	91.9	58.0	44.6	68.2	51.6	56.1	39.7	89.1
	GRASS	98.4	96.1	89.8	97.7	94.2	83.0	96.7	100.0
	HIBU	86.9	79.6	96.7	89.7	88.7	90.2	95.5	89.6
	TREE	98.4	99.6	98.2	98.9	98.5	98.3	99.4	96.7
2018	WATER	35.7	100.0	97.3	100.0	100.0	100.0	98.2	100.0

Our results showed that NN had the highest overall accuracy, average PA and UA for all the analysis years. SVM and RF closely followed NN and also showed accurate classification results. ML successfully classified the image but had lower accuracy compared to the machine learning algorithms tested.

Land Cover Change

All the algorithms successfully classified the land cover for 2009, 2014 and 2018 but we decided to use NN for the land cover change analysis because it has the highest overall accuracy, PA and UA. The graph of land cover classification area computation show the increasing trends in built-up area and soil and decline in grass,

tree and surface water coverage (Table 4 and Figure 2). The 49% tree-covered area of the study site in 2009 and declined to 43% in 2018 as built-up area starting at 32% expanded to 42%. In Figure 3, the spread of built-up area first to the north and then to the east and south across time is illustrated.

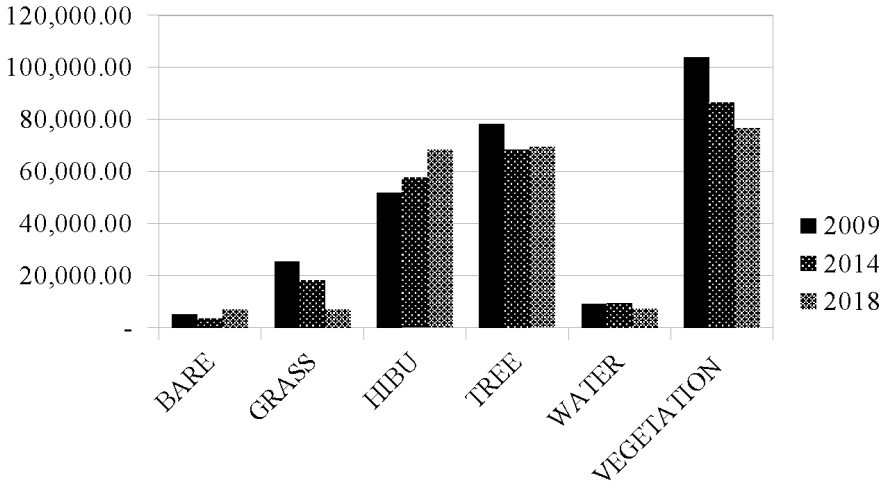

Figure 2: Land cover area computation (2009, 2014 and 2018)

Table 4: Land cover change area

Class	Area (sq.km)			%		
	2009	2014	2018	2009	2014	2018
Bare	19.68	35.72	68.37	1.23	2.23	4.26
Grass	180.07	181.22	69.72	11.23	11.30	4.35
Built	521.07	578.94	686.52	32.50	36.11	42.82
Tree	784.15	683.67	696.16	48.91	42.64	43.42
Water	91.98	94.68	73.41	5.74	5.91	4.58
Others	6.28	29.01	9.06	0.39	1.81	0.56
Total	**1,603.24**	**1,603.24**	**1,603.23**	**100.00**	**100.00**	**100.00**

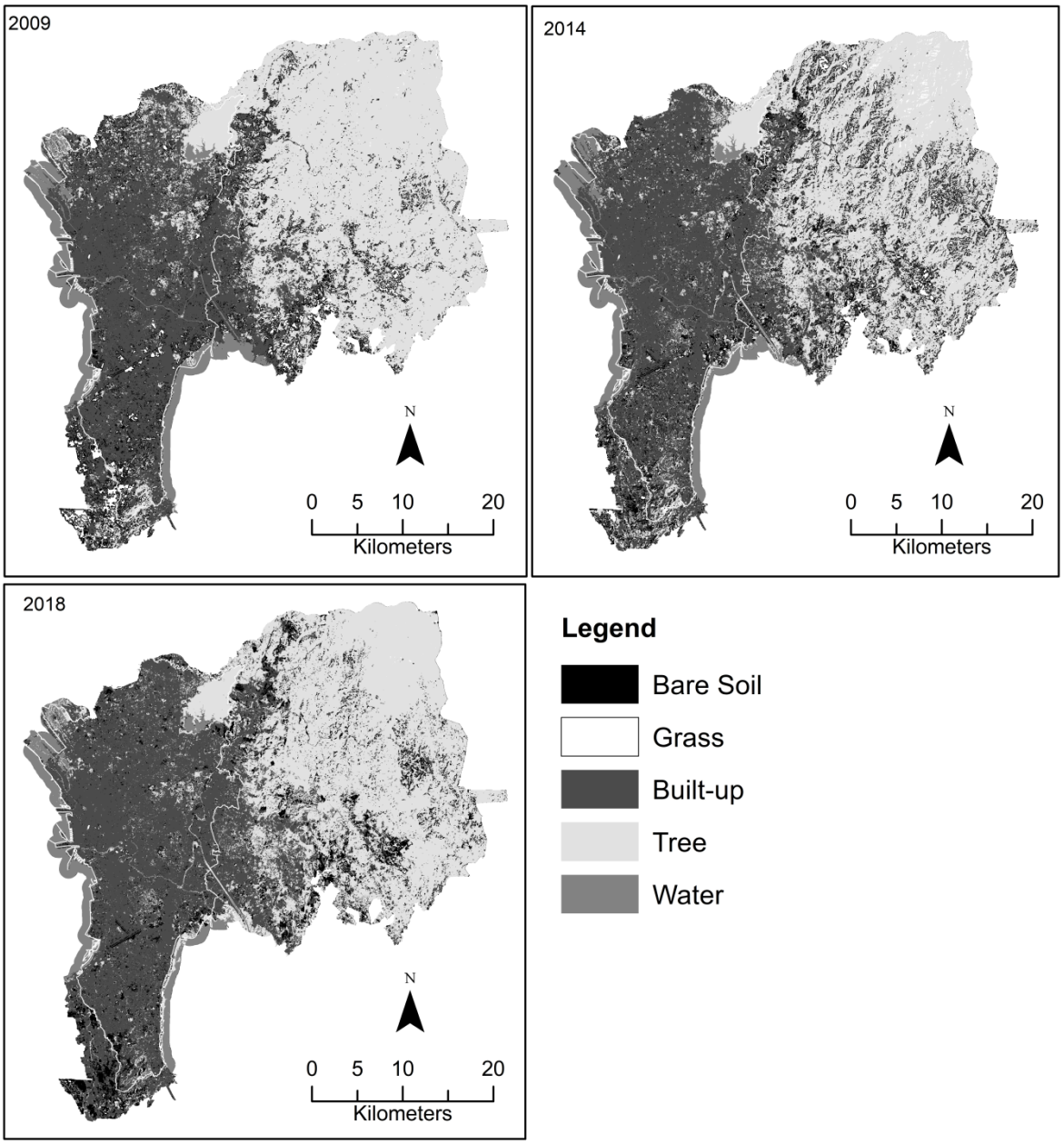

Figure 3: Land cover classification of 2009, 2014, and 2018

Land Cover Transition: Urban Expansion

Our estimation (Table 5) revealed that more than 77% (1,239 km^2) in 2009-2014 and 79% (1,244 km^2) in 2014-2018 of the study site remained unchanged. In the remaining area that experienced change, major changes observed were urban expansion and transition in vegetation-covered surfaces. In 2009-2014 period, urban expansion happened in grasslands (53.9 km^2), tree (47.9km^2), bare soil (12.1km^2) and water (2.1 km^2). In 2014-2018 period, 82.1 km^2 of tree-covered surfaces, 37.1 km^2 of grasslands, 27.2 km^2 of bare soil and 6.5 km^2 of surface water were converted to built surface. Built-up expansion grew more extensive and intensive in the later time period. The computed annual rate of change also reveal that the transition to urban surface more

than doubled in 2014-2018 (26.9 km^2/year) compared with 2009-2014 period (11.5 km^2/year). This estimate was close to the estimates of Faraon, et al., (2016). In their study, they compared the built-up areas of 2003 and 2010 from NAMRIA over the larger Laguna Watershed covering Marikina Watershed, Metro Manila and other watersheds draining to Laguna Lake and estimated the annual urban growth of more than 11%. IN this time period, built-up expansion was observed in the northeastern and southwestern open spaces. In the next period (2014-2018), built-up conversion was still evident in between the urban spaces but greater development was happening outside the main city towards the east. In 2018, almost all the green space in Metro Manila are gone and patches of urban spaces outside Metro Manila grew.

Vegetation Loss and Recovery

Built-up expansion translates to vegetation loss. In 2009-2014, the study site lost 165.4 km^2 (21.1%) land covered with trees and gained only 64.4 km^2 (9.4%). In this period, our estimations show that for every 1 km^2 of tree-covered area gained, 3 km^2 of tree-covered area was lost and that the tree-covered land loss rate (20.2 km^2/year) was twice the rate of urban development (11.5km^2/year).

If compared with other research, our estimates vary due to the study site coverage difference. However, other researchers also observed the same trend of vegetation loss or deforestation in the Marikina Watershed for study periods prior to 2014. Albino, et al. (2015) conducted a study comparing land cover in 1999 and 2006 and observed deforestation in Marikina Watershed. They observed a decrease in forest cover from 108 km^2 in 1999, forest cover shrunk to 104 km^2 in 2006 (Albino, et al., 2015). In another study, Brebante (2017) computed a decline in Marikina Watershed's forest cover from 187 km^2 in 1989, forest cover area dropped to 134 km^2 in 2016 (Brebante, 2017). In 2003-2010, increase in grassland area and decrease in forest area were also observed by Faraon, et al., (2016). They attributed this loss to agriculture activities especially in the higher elevations. They mentioned that forest in this region has decreased from 53% to 8% in five decades starting 1940 with logging activities reaching its peak in the 1970 urban development, extraction and trade of forest goods. To better understand the causes of vegetation loss, we plotted the MPSA locations and observed vegetation loss inside those locations especially in the 2014-2018 period.

In contrast to the consistent vegetation loss reported by previous research, our results found out that after 2014, tree-covered areas expanded by 117.9 km^2 (16.9%) while losing 105.4 km^2 (15.4%). On the average, tree-covered areas expanded by 3.1 km^2 per year in 2014-2018. This was not observed in previous studies due to differences in spatial coverage, time period and intervals.

Two years after the flood event of Tropical Storm Ketsana in September 2009, tree planting activities for the National Greening Program (EO 26, 2011) which is a nationwide program aiming to plant more than a billion trees started and the Marikina Watershed Reservation was proclaimed as the Upper Marikina River Basin Protected Landscape (Presidential Proclamation No. 296). In our study site, around 230 km^2 of land were covered in the NGP from 2011 to 2016. During 2009-2014 period, transition to trees happened mostly outside the NGP sites. Out of the total 190 km^2 mapped NGP sites from 2011 to 2014, only 1.68 km^2 (0.88%) was detected to have conversion to tree cover in 2014. The transition matrix show that for the 2014-2018 time period, 73.8 km^2 of grasses were converted to trees. Only 23.5 km^2 of land cover conversion to trees were detected inside the total area of NGP sites starting in 2011. The results of the reforestation program did not immediately show on the maps and took years to manifest. It would take more years for new trees to grow and see the impact of the greening program on the landscape.

Despite the reforestation program, decline in tree-covered areas persist and they happen even inside the Upper Marikina River Basin Protected Landscape and inside the NGP sites. This implies that greater emphasis and effort should be given to protection and preservation of tree cover in watershed. Removal of vegetation takes less time but once tree cover was removed it would take years for the trees to recover.

Table 5: Land cover transition matrix

	2009-2014					2014-2018				
LAND COVER	BARE	GRASS	BUILT	TREE	WATER	BARE	GRASS	BUILT	TREE	WATER
AREA1 (sqkm)	24.4	180.2	521.2	784.7	92.2	35.7	181.2	578.9	683.7	94.7
AREA2 (sqkm)	35.7	181.2	578.9	683.7	94.7	68.4	69.7	686.5	696.2	73.4
CHANGE (sqkm)	11.3	1.0	57.7	-101.0	2.5	32.7	-111.5	107.6	12.5	-21.3
NO CHANGE (sqkm)	2.8	72.4	461.8	619.3	83.4	6.7	49.0	523.4	578.3	71.6
Change to BARE (SQKM)		6.7	22.7	3.0	0.3		21.2	25.2	8.7	2.9
Change to GRASS (SQKM)	2.0		7.3	98.9	0.5	0.7		5.5	12.7	0.2
Change to BUILT (SQKM)	12.1	53.9		47.9	2.1	27.2	37.1		82.1	6.5
Change to TREE (SQKM)	1.9	38.1	18.3		5.4	0.6	73.8	22.0		8.4
Change to WATER (SQKM)	0.6	0.3	5.2	2.6		0.2	0.0	0.7	0.7	
GAIN (sqkm)	32.9	108.8	117.1	64.4	11.3	61.7	20.7	163.1	117.9	1.8
GAIN (%)	92.1	60.0	20.2	9.4	12.0	90.2	29.8	23.8	16.9	2.4
LOSS (sqkm)	21.6	107.8	59.4	165.4	8.8	29.0	132.2	55.5	105.4	23.1
LOSS (%)	88.5	59.8	11.4	21.1	9.6	81.2	73.0	9.6	15.4	24.3
ANNUAL RATE OF CHANGE (SQKM/YEAR)	2.3	0.2	11.5	-20.2	0.5	8.2	-27.9	26.9	3.1	-5.3

Conclusions and Recommendations

This paper showed general land cover classification performed successfully using supervised pixel-based algorithms. All the four algorithms yielded satisfactory land cover classification results in this urbanized and urbanizing metropolitan region and its adjacent watersheds. This classification scheme produced seven classes

including bare soil, grass, built, tree, water, clouds and shadows. Neural Network and Random Forest, closely followed by Support Vector Machines were able to produce the most accurate results. All of the classifiers had a difficulty in correctly classifying bare soil due to soil spectra, the shadows and the type of soil in the area collected as training pixel. All of them accurately classified built-up, trees and water. The image quality, particularly the presence of clouds and the number of training pixels were the primary factors influencing the accuracy of the classifiers. Further studies would be necessary to address those factors.

Less than 33% of the study site experienced changes in land cover during from 2009 to 2018. Built-up areas expanded at first filling the spaces within Metro Manila. More recent images show that built-up areas expand towards the northeast and southwest in 2009-2014 and are not moving towards the east in 2014-2018. The rate of urban expansion sped up in the last four years to 26.9 km^2 per year from 11.5 km^2 per year in 2009-2014. Anthropogenic activities particularly urban development, agriculture and mining influenced land cover change causing a general reduction in vegetal coverage especially and continued increase in impervious surface. Tree cover decreased in the period of 2009-2014 and slightly increased in 2014-2018. The increase in tree cover was aided by reforestation programs but is also hindered by urban development, mineral extraction and crop production. This calls for preservation and protection of the tree cover in the watershed. This study did not study the species of plants used for reforestation programs. Further studies should be done to assess the appropriateness of those tree species planted for reforestation. The watershed needs more intensive protection while it is recovering. This requires strengthening of the implementation of the UMRB Protected Landscape law. This also calls for equitable land use planning for the watershed and proper implementation for sustainable resource use as less space becomes available for the competing demands.

References

Abdulkareem, J., Pradhan, B., Sulaiman, W., & Jamil, N. (2017). Prediction of spatial soil loss impacted by long-term land-use/land-cover change in a tropical watershed. *Geoscience Frontiers*, 1-15.

Ahmad, A., & Quegan, S. (2012). Analysis of Maximum Likelihood Classification on Multispectral Data. *Applied Mathematical Sciences*, 6425-6436.

Albino, A. C., Kim, S. Y., Jang, M. N., Lee, Y. J., & Chung, J. S. (2015). Assessing land use and land cover of the Marikina sub-watershed, Philippines. *Forest Science and technology*, 1-11.

Bankoff, G. (2003). *Cultures of Disaster: Society and natural hazard in the Philippines.* New York: RoutledgeCurzon.

Belgiu, M., & Dragut, L. 2015. Random Forest in Remote Sensing: A Review of Applications and Future Directions. ISPRS Journal of Photogrammetry and Remote Sensing, 114, 24-31.

Bhat, P. A., Shafiq, M., Mir, A. A., & Ahmed, P. (2017). Urban sprawl and its impact on landuse/land cover dynamics of Dehradun City, India. *International Journal of Sustainable Built Environment*, 513-521.

Blanco, A., & Nadaoka, K. (2006). A comparative assessment and estimation of potential soil erosion rates and patterns in Laguna Lake watershed using three models: towards development of an erosion index system for integrated watershed-lake management. *Paper presented at: Symposium on Infrastructure Development and the Environment; SEA-MEO_INNOTECH, University of the Philippines, Diliman, Quezon City, PHilippines*.

Boongaling, C. K., Faustino-Eslava, D. V., & Felino, L. P. (2018). Modeling land use change imapcts on hydrology and the use of landscape metrics as tools for watershed management: The case of an ungauged catchment in the Philippines. *Land Use Policy*, 116-128.

Brebante, Beverly Mae. 2017. Analyzing the Effects of Land Cover/Land Use Changes on Flashflood: A Case Study of Marikina River Basin (MRB), Philippines. University of Twente, Enschede, Netherlands.da

Dalu, M. T., Shackleton, C. M., & Dalu, T. (2018). Influence of land cover, proximity to streams and household topographical location on flooding impact in informal settlements in the Eastern Cape, South Africa. *International Journal of Disaster Risk Reduction*, 481-490.

Deilmai, B., Ahmad, B., & Zabihi, H. (2014). Comparison of two classification methods (MLC and SVM) to extract land use and land cover in Johor Malaysia. *IOP Conf. Ser.: Earth Environ, Sci.* IOP.

Estoque, R.C., Lasco, R.D., Myint, S.W., Pulhin, F.B., Wang, C., Ooba, M., Hijoka, Y. 2018. Changes in the landscape pattern of the La Mesa Watershed–The last ecological frontier of Metro Manila, Philippines. Forest Ecology and Management, **430**, 280-290.

Faraon Alvin a., Adelina C. Santos-Borja, Neil V. Varcas, Brando M. Angeles, Erwin Kim P. Mercado. 2016. Valuation of Ecosystem Service of the Laguna Lake Basin: Erosion Control and Flood Water Retention. https://www.pref.ibaraki.jp/soshiki/seikatsukankyo/kasumigauraesc/04_kenkyu/kaigi/docments/kosyou/16/2016wlc_alvin_faraon.pdf Forster, B. 1983. Some urban measurements from Landsat data. Photogrammetric Engineering and Remote Sensing 49, 1293-1707.

Forster, B.C. 1985 An examination of some problems and solutions in monitoring urban areas from satellite platforms. International Journal of Remote Sensing, 6, 139-151.

Gashaw, T., Tulu, T., Argaw, M., & Worqlul, A. W. (2018). Modeling the hydrological impacts of land use/land cover changes in the Andassa watershed, Blue Nile Basin, Ethiopia. *Science of the Total Environment*, 1394-1408.

Griffiths, R., Hostert, P., Gruebner, O. & van der Linden, S. 2010. Mapping megacity growth with multi-sensor data. Remote Sensing of Environment 114, 426-439.

Grimm , N., Grove , J., Picket, S., & Redman, C. (2000). Integrated approaches to long-term studies of urban ecological systems. *Bioscience*.

Grimm, N., Faeth, S., Golubiewski, N., Redman, C., Wu, J., & Bai, X. (2008). Global change and the ecology of cities. *Science*, 756-760.

Housing and Land Use Regulatory Board. 1997. Guidelines for the Formulation/Revision of a Comprehensive Land Use Plan: Local Administration, Vol. X. Quezon City: HLURB. Hsu CW, Change CC, Lin CJL (2010) Practical guide to support vector classification. Available at: http://www.csie.ntu.edu.tw/-cjlin . Accessed 26 May 2015.

Immitzer, Markus, Clement Atzberger. 2012. Tree species classification with random forest using very high spatial resolution 8-band WorldView-2 satellite data. Remote Sensing 4(9).

Jimenez, A., Vilchez, F., Gonzales, O., & Marceleno Flores, S. (2018). Analysis of the Land Use and Cover Changes in the Metropolitan Area of Tepic_Xalisco (1973-2015) through Landsat Images. *Sustainability*.

Kanellopoulos, I., Wilkinson G.G. 1997. Strategies and best practice for neural network image classification. International Journal of Remote Sensing, 18 (4), pp. 711-725.Karan, S., & Samadder, S. (2018). A comparison of different land-use classification techniques for accurate monitoring of degraded coal-mining areas. *Environmental Earth Sciences*, 712-727.

Klein, R. (1979). Urbanization and stream quality impairment. *J. Am. Water Resour. Assoc.*, 948-963.

Lei, C., & Zhu, L. (2018). Spatio-temporal variability of land use/land cover change (LULCC) within the Huron River: Effects on stream flows. *Climate Risk Management*, 35-47.

Leopold , L. (1968). *Hydrology for urban land planning: A guidebook on the hydrologic effects of urban land use.*

Li, J., Wang, X., Ma, M., & Zhang, H. (2009). Remote Sensing evaluation of urban heat island and its spatial pattern of the Shanghai metropolitan area,. *China Ecol. Complex.*, 413-420.

Lopez, E., Bocco, G., Mendoza, M., Duhau, E., 2001. Predicting land cover and land-use change in the urban fringe: a case in Morelia city, Mexico. Landscape Urban Planning, 55.

Meng, X., Currit, N., Wang, L., & Yang, X. (2010). Object-oriented residential building land use mapping using Lidar and Aerial Photographs. *ASPRS 2010 Annual Conference.* San Diego.

Moran, M., Jackson, R., Slater, P., & Teillet , P. (1992). Evaluation of simplified procedures for retrieval of land surface reflectance factors from satellite sensor output. *Remote Sensing of Environment, 41*, 169-184.

Murayama, Y., Estoque, R. C., Subasinghe, S., Hou, H., & Gong, H. (2015). Land-Use/Land-Cover Changes in Major Asian and African Cities. *Annual report on the multi use social and economic data bank*.

Mushore, T., Mutanga, O., Odindi, J., & Dube, T. (2017). Linking major shifts in land surface temperatures to long term land use and land cover changes: A case of Harare, Zimbabwe. *Urban Climate*, 120-134.

Namugize, J. N., Jewitt, G., & Graham, M. (2018). Effects of land use and land cover changes on water quality in the uMngeni river catchment, South Africa. *Physics and Chemistry of the Earth*.

Noi, P.T. & Kappas, M. 2017. Comparison of Random Forest, k-Nearest Neighbor, and Support Vector Machine Classifiers for Land Cover Classification Using Sentinel-2 Imagery. Sensors, 18.

Petropoulos, G., Griffiths, H., & Kalivas, D. (2014). Quantifying spatial and temporal vegetation recovery dynamics following a wilffire event in a Mediterranean landscape using EO data and GIS. *Appl. Geogr.*, 120-131.

Priyadarshini, K., Kumar, M., Rahaman, S., & NiteshNirmal, S. (2018). A Comparative Study of Advanced Land Use/Land Cover Classification Algorithms Using Sentinel-2 Data. *ISPRS TC V Mid-term Symposium "Geospatial Technology - Pixel to People"*. Dehradun, India.

Richards, J.A. 1999. Remote Sensing Digital Image Analysis Berlin: Springer-Verlag, 240 pp.

Richards JA, Jia X. 2006. Remote sensing digital image analysis-hardback. Springer, Berlin.

Ustuner, Mustafa, Fusun Balik Sanli, Barnali Dixon. 2015. Application of Support Vector Machines for Landuse Classification Using High-Resolution RapidEye Images: A Sensitivity Analysis. European Journal of Remote Sensing 48: 403-422.

Sajikumar, N., & Remya, R. (2015). Impact of land cover and land use change on runoff characteristics. *Journal of Environmental Management*, 460-468.

Sharma, Atharva, Xiuwen Liu, Xiaojun Yang. 2018. Land cover classification for multi-temporal, multi-spectral remotely sensed imagery using patch-based recurrent neural networks. Neural Networks. 346-355.Sun, L., Wei, J., Duan, D., Guo, Y., Yang, D., Jia, C., & Mi, X. (2016). Impact of land-use and land-cover change on urban air quality in representative cities of China. *J. Atmos. Solar-Terr. Phys.*, 43-54.

Small, C. 2005. A global analysis of urban reflectance. International Journal of Remote Sensing, 26, 661-681.

Taubenbock, H., Esch, T., Felbier, A., Wiesner, M., Roth, A., & Dech, S. (2012). Monitoring urbanization in mega cities from space. *Remote Sensing of Environment*, 162-176.

Toure, S. I., Stow, D. A., Shih, H.-c., Weeks, J., & Lopez-Carr, D. (2018). Land cover and land use change analysis using multi-spatial resolution data and object-based image analysis . *Remote Sensing of Environment*, 259-268.

Weng, Q., & Liu , D. 2007. Subpixel analysis of urban landscapes. Urban remote sensing: CRC Press.

Wu, C., & Murray, A. (2003). Estimating impervious surface distribution by spectral mixture analysis. *Journal of Remote Sensing of Environment*, 493-505.

Yang, Xiaojun. 2011. Parameterizing Support Vector Machines for Land Cover Classification. Photogrammetric Engineering & Remote Sensing. Vol. 77. No. 1. pp. 27-37.

Ye, X., Yu, X., Yu, C., Tayibazhaer, A., Xu, F., Skidmore, A., & Wang , T. (2018). Impacts of future climate and land cover changes on threatened mammals in the semi-arid Chinese Altai Mountains. *Science of the Total Environment*, 775-787.

Zhou, X., & Chen, H. (2018). Impact of urbanization-related land use and land cover changes and urban morphology changes on the urban heat island phenomenon. *Science of the Total Environment*, 1467-1476.

Zoleta-Nantes, D. B. (2000). Flood Hazards in Metro Manila: Recognizing Commonalities, Differences, and Courses of Action. *Social Science Diliman*, 60, 1.